

Chapter 11

Discussion on Specificity of Molecular Signals in Response to Certain Environmental Toxicants or Stresses



Abstract In the field of toxicology or environmental science, some researchers are wondering a question. That is, whether specific molecular signaling pathways in response to certain environmental toxicants or stresses exist in organisms. We selected three well-described response signals (heavy metal response, heat shock response, and hypoxia response) to discuss this question. So far, the obtained knowledge does not support the possible existence of specific molecular signaling pathways in response to certain environmental toxicants or stresses at least in nematodes.

Keywords Heavy metal response signaling · Heat shock response signaling · Hypoxia response signaling · Specific molecular signaling · *Caenorhabditis elegans*

11.1 Introduction

In the environment, there are many toxicants or stresses having the potential to cause the toxicity at different aspects on nematodes [1–6]. For a long time, the researchers in the field of toxicology or environmental science have tried to identify the specific molecular signaling pathways for nematodes in response to certain environmental toxicants or stresses. And then, an important question needs us to further carefully judge or evaluate. That is, are there any specific molecular signals for nematodes in response to certain environmental toxicants or stresses?

In this chapter, we selected three well-described response signals (heavy metal response, heat shock response, and hypoxia response) to discuss this question. We first introduced and discussed the widely accepted molecular signals for the control of these three important responses. Again, we will discuss the potential involvement of these molecular signals in the regulation of toxicity from other environmental toxicants or stresses in nematodes.

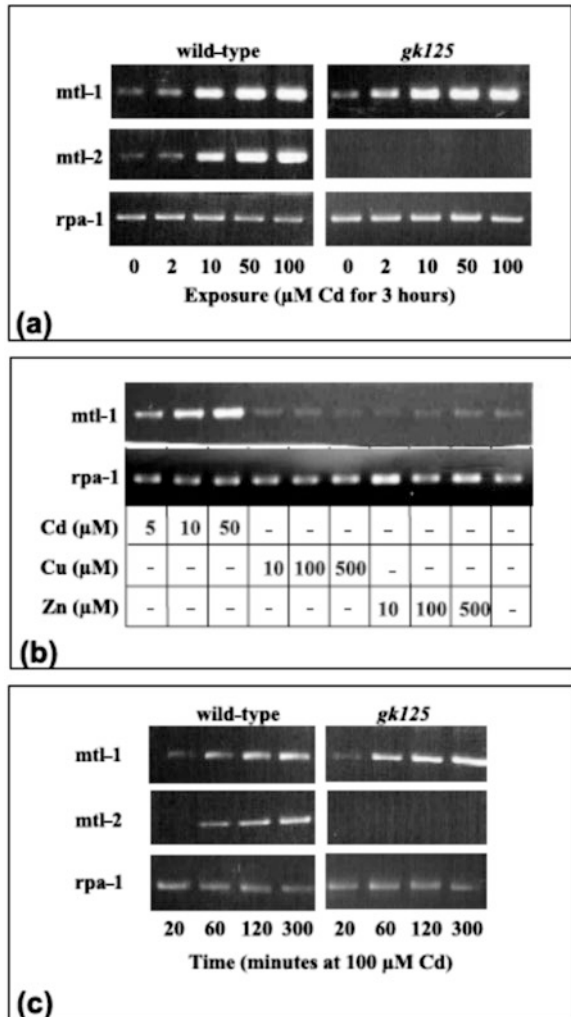
11.2 Heavy Metal Response Signaling

11.2.1 Molecular Signaling for Heavy Metal Response

11.2.1.1 Metallothioneins

Metallothioneins are widely considered as the primary player in the detoxification of and protection from toxicity by the heavy metal of cadmium (Cd) [7]. In nematodes, *mtl-1* and *mtl-2* encode the metallothioneins. A highly sensitive and dose-dependent transcriptional response to Cd, but not Cu or Zn, was observed for both MTL-1 and MTL-2 (Fig. 11.1) [7]. Additionally, Cd exposure induced the

Fig. 11.1 Isoform-specific transcript analysis of *mtl-1* and *mtl-2* [7]. Utilizing a semiquantitative PCR-based approach, it was possible to assess the dose response to cadmium (a), copper, and zinc (b) and the temporal response to cadmium exposure (c) of *mtl-1* and *mtl-2* in wild-type nematodes and *gk125* the *mtl-2* null allele. PCRs were terminated at the half-log phase of amplification and normalized to the invariant ribosomal protein *rpa-1*



sharp induction of both MTL-1::GFP in the pharynx and intestine and MTL-2::GFP in the intestine (Fig. 11.2) [7]. No measurable upregulation of *mtl-1* could be detected in *mtl-2* mutant nematodes [7], suggesting that these two genes are independent and not synergistic action may be formed.

Mutation or RNAi knockdown of *mtl-1* or *mtl-2* induced a susceptibility to Cd toxicity using body size, generation time, brood size, and lifespan as the toxicity assessment endpoints (Fig. 11.3) [7], which provide the functional evidence to demonstrate the important roles of MTL-1 and MTL-2 in regulating the Cd toxicity in nematodes.

11.2.1.2 CDR-1

CDR-1 is a predicted 32-kDa, integral membrane protein. *cdr-1* is transcribed exclusively in intestinal cells of postembryonic nematodes [8]. In the intestine, the CDR-1 is targeted to the cytoplasmic lysosomes [8]. The *cdr-1* transcription was

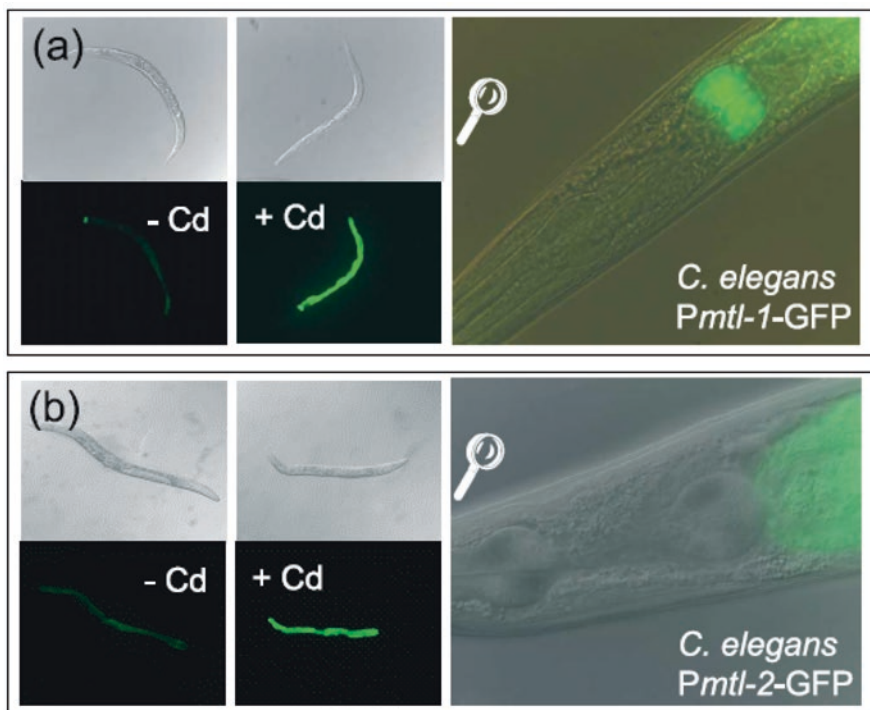


Fig. 11.2 Promoter-GFP fusions of *mtl-1* (a) and *mtl-2* (b) after germ line transformation [7]. The background signal (-Cd) was significantly increased by exposure to 10 mM cadmium (+Cd) for a 24 h period. In both isoforms, the primary site of cadmium responsive induction is the intestine, but note that only *mtl-1* is expressed constitutively in the lower pharyngeal bulb (right-hand panels)

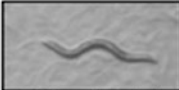

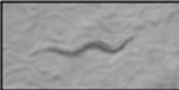


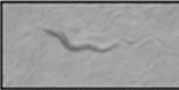
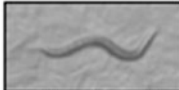




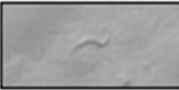
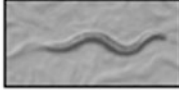


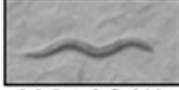
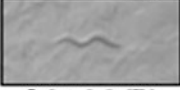

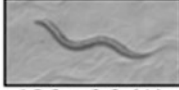
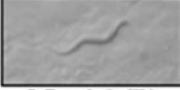

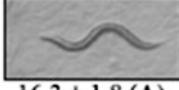


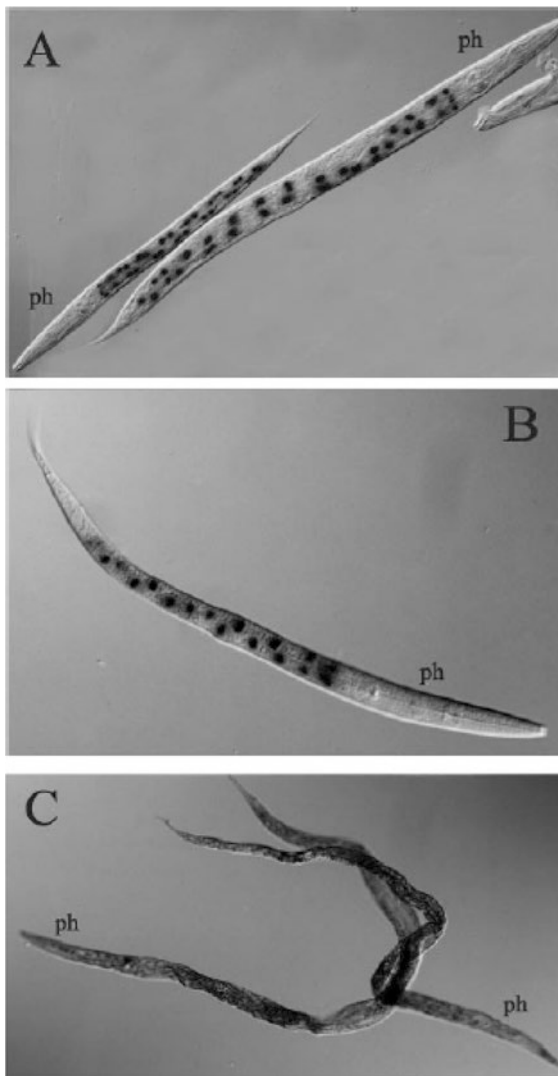
worm strain	RNAi source	cadmium concentration (μM)		
		0	75	150
wild-type	pPD129.36	 15.2 ± 1.1 (A)	 11.7 ± 0.4 (B)	 7.9 ± 0.8 (C)
<i>rff-3</i>	pPD129.36	 14.1 ± 0.8 (A)	 11.4 ± 0.3 (B)	 8.3 ± 0.7 (C)
<i>rff-3</i>	<i>mtl-1</i>	 13.1 ± 1.9 (A)	 5.1 ± 0.5 (D)	 3.5 ± 0.7 (D)
<i>gkl25</i>	<i>mtl-1</i>	 16.6 ± 0.6 (A)	 6.1 ± 0.5 (D)	 2.0 ± 0.4 (E)
<i>rff-3</i>	<i>mtl-2</i>	 15.4 ± 0.3 (A)	 4.7 ± 0.4 (D)	 4.9 ± 0.3 (D)
<i>gkl25</i>	<i>mtl-2</i>	 16.8 ± 1.3 (A)	 5.6 ± 0.9 (D)	 3.0 ± 1.0 (E)
<i>rff-3</i>	<i>mtl-1+2</i>	 15.2 ± 2.3 (A)	 5.7 ± 0.8 (D)	 4.5 ± 0.6 (D)
<i>gkl25</i>	<i>mtl-1+2</i>	 16.3 ± 1.8 (A)	 5.9 ± 0.8 (D)	 3.3 ± 0.3 (E)

Fig. 11.3 Exposure to cadmium slows down development in a dose-responsive manner [7]. This effect is more profound in *gkl25* and particularly during knockdown of *mtl-1*, *mtl-2*, or both by RNAi. All images are representative of 2-day post hatch nematodes. Numbers below the images are average area measurements (G standard error) from four nematodes. Based on a nonparametric Mann–Whitney U-test, identical letters (in brackets) denote that samples are not significantly different ($P \geq 0.05$)

Fig. 11.4 Cell-specific expression of *cdr-1* [8]. (a, b) *C. elegans*, strain JF9 (*mtIs7, cdr-1/lacZ*) was exposed to 100 μM CdCl_2 for 24 h and then stained for β -galactosidase activity. (a) Reporter gene activity in the intestinal cells of a young adult and an L3 larva. (b) *cdr-1* promoter activity in the intestinal cells of an L1 larva. (c) In situ hybridization of cadmium-treated L1 *C. elegans* larvae. CDR-1 mRNA was visualized by exposing wild-type nematodes to a digoxigenin-dUTP-labeled CDR-1 antisense probe. (c) shows that the CDR-1 transcript is expressed throughout the intestine of L1. “*ph*” marks the location of the pharynx in all panels. Nematodes were photographed using Nomarski optics



significantly induced by Cd exposure, but not by other examined stressors (heavy metals of Hg, Cu, and Zn, paraquat, hugalone, and heat shock) (Fig. 11.4) [8], suggesting that CDR-1 expression is under the control of Cd exposure in a cell-specific fashion. In addition, RNAi knockdown of *cdr-1* also induced a susceptibility to Cd [8, 9].

11.2.2 Regulation of Toxicity of Other Environmental Toxicants by *MTL-1* and *MTL-2*

Some engineered nanomaterials (ENMs) have been shown to be toxic for organisms, including the nematodes [10–17]. Among these ENMs, titanium dioxide nanoparticles (TiO₂-NPs) and zinc oxide NPs (ZnO-NPs) are two widely used ENMs. In nematodes, mutation of *mtl-2* resulted in a susceptibility to the TiO₂-NPs toxicity in reducing body length, in reducing brood size, in decreasing locomotion behavior as indicated by the endpoints of head thrash and body bend, and in inducing intestinal autofluorescence and ROS production [18]. In nematodes, *pcs-1* encodes a phytochelatin synthase. Additionally, the severe susceptibility to ZnO-NPs toxicity was observed in the triple mutant of *mtl-1;mtl-2;pcs-1(zs2)* (Fig. 11.5) [19]. Moreover, the *mtl-2::GFP* expression was significantly increased by exposure to ZnO-NPs in nematodes (Fig. 11.5) [19].

Nanopolystyrene particles are another important ENM with the wide commercial uses. In nematodes, prolonged exposure to nanopolystyrene particles caused the toxicity on the functions of both primary and secondary targeted organs [20]. It was further found that the intestinal insulin signaling pathway including the *daf-16* encoding a FOXO transcriptional factor was involved in the control of toxicity of nanopolystyrene particles [21]. *daf-16* has many potential targeted genes during the control of biological processes [22–24], and, among them, *lys-8*, *dct-6*, *nnt-1*, *ftn-1*, *pept-1*, *dod-17*, *klo-1*, *ncx-6*, *cyp-35A3*, *nhx-2*, *vha-6*, *pho-1*, *gale-1*, *cyp-34A9*, *stdh-1*, *nrf-6*, *hsp-16.1*, *hsp-16.2*, *asah-1*, *ges-1*, *cpr-1*, *acd-1*, *vit-5*, *mtl-2*, *dod-22*, *gcy-18*, *vit-2*, *lys-7*, *mtl-1*, *dct-18*, *gpb-2*, *fat-5*, *cyp-35B1*, *sod-3*, *sodh-1*, *icl-1*, *fat-7*, *dod-4*, *fat-7*, *asp-3*, *mdl-1*, *spp-1*, and *dct-1* can be expressed in the intestine. Exposure to nanopolystyrene particles (1 µg/L) only significantly increased the transcriptional expressions of *sod-3*, *mtl-1*, *gpb-2*, *fat-7*, and *sodh-1* in wild-type nematodes (Fig. 11.6) [21]. Meanwhile, *daf-16* mutation significantly decreased the transcriptional expressions of *sod-3*, *mtl-1*, *gpb-2*, *fat-7*, and *sodh-1* after exposure to nanopolystyrene particles (1 µg/L) (Fig. 11.6) [21]. Among these targeted genes, using VP303 as a genetic tool, it was observed that intestine-specific RNAi knockdown of *mtl-1* induced a susceptibility to the toxicity of nanopolystyrene particles in inducing ROS production (Fig. 11.6) [21]. These results suggest that *mtl-1* acts as a targeted gene of *daf-16* in the regulation of toxicity of nanopolystyrene particles.

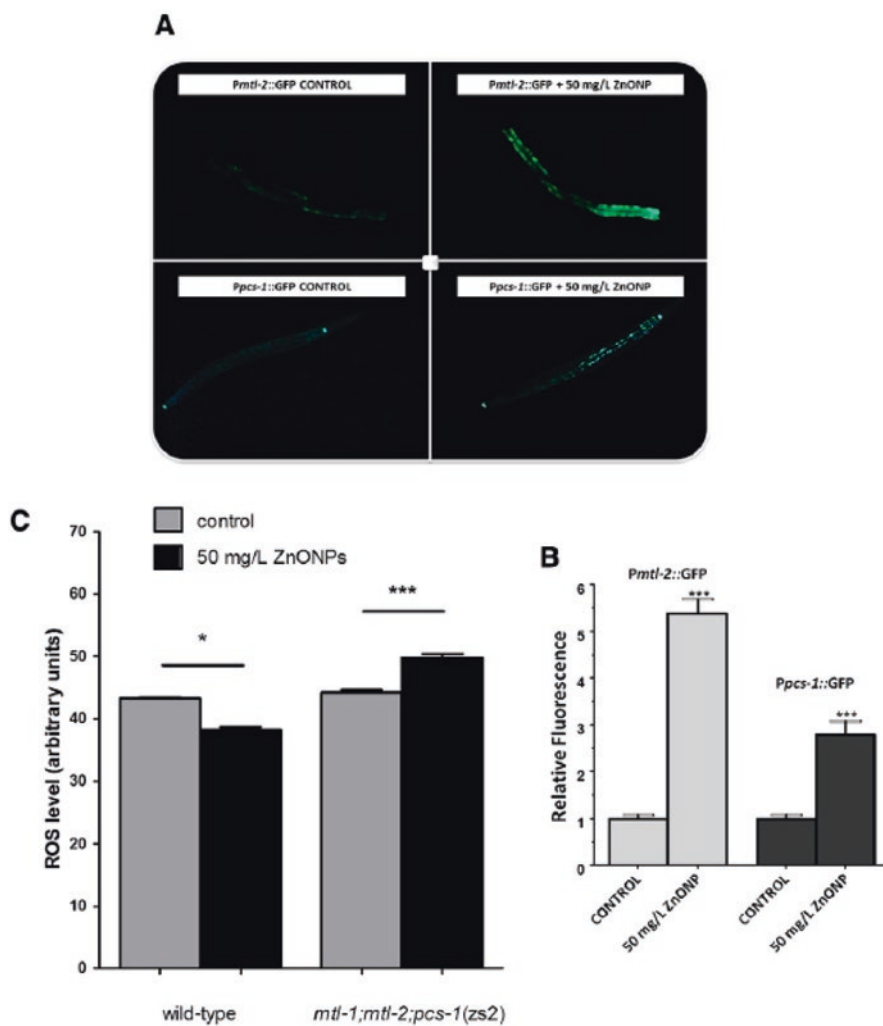


Fig. 11.5 Induction of green fluorescence protein (measured as relative fluorescence units) in *mtl-2::GFP* and *pcs-1::GFP* transgenic *Caenorhabditis elegans* in response to ZnO-NPs [19]. Approximately ten worms were observed in each case. Error bars represent the standard error ($n = 10$). Statistical analysis was performed using the Wilcoxon signed-rank test ($p < 0.05$). Exposure to ZnO-NPs generates high levels of free radical H_2O_2 in *C. elegans*.

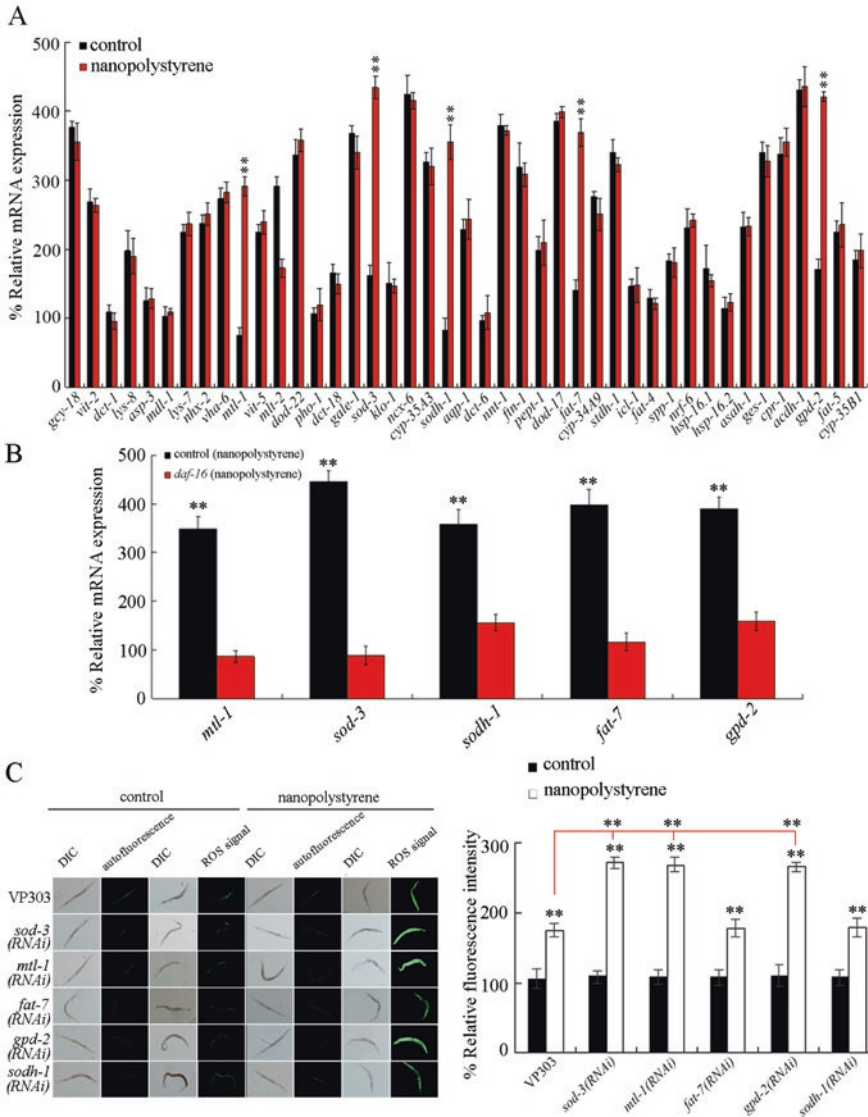


Fig. 11.6 Identification of targeted genes for *daf-16* in the regulation of response to nanopolystyrene particles [21]. (a) Effects of exposure to nanopolystyrene particles on gene expression in wild-type nematodes. (b) Effects of *daf-16* mutation on expression of intestinal targeted genes of *daf-16* after exposure to nanopolystyrene particles. (c) Effect of intestine-specific RNAi knock-down of *sod-3*, *mtl-1*, *gpd-2*, *fat-7*, or *sodh-1* on induction of ROS production in nematodes exposed to nanopolystyrene particles. Nanopolystyrene exposure concentration was 1 $\mu\text{g/L}$. Nanopolystyrene exposure was performed from L1-larvae to adult day 3. Bars represent means \pm SD. $**P < 0.01$ vs control (if not specially indicated)

11.3 Heat Shock Response Signaling

11.3.1 Molecular Signaling for Heat Shock Response

11.3.1.1 Heat Shock Proteins

Early in 1983, it was reported that treatment of the nematodes with elevated temperatures could induce the synthesis of the heat shock proteins [25]. In contrast, synthesis of most other proteins present before the heat shock was suppressed [25]. Additionally, the dauer larvae possess little translatable mRNA but, upon the heat shock, synthesizes a set of messages corresponding to the heat shock proteins [25].

11.3.1.2 HSF-1

hsf-1 encodes a heat shock factor. HSF-1 is a master transcriptional regulator of stress-inducible gene expression, as well as protein-folding homeostasis [26]. *hsf-1* was required for both the longevity control and the temperature-induced dauer larvae formation in nematodes [26, 27]. Heat shock-induced expression of *hsp-16.2* was virtually eliminated in *hsf-1* mutant nematodes (Fig. 11.7) [27], suggesting the potential role of HSF-1 as an inducer of heat shock response.

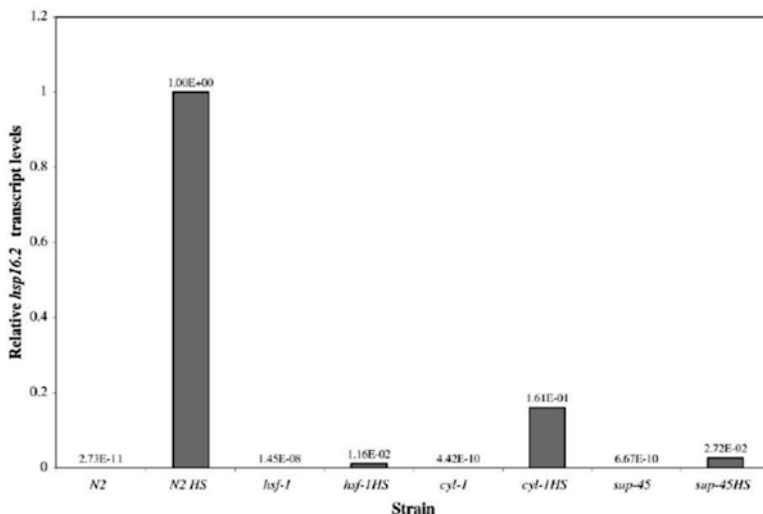


Fig. 11.7 Decreased levels of *hsp-16.2* mRNA in suppressor mutants, as measured by quantitative real-time PCR [27]. Input levels for each sample were normalized with control PCR reactions using 18S rRNA

11.3.2 Regulation of Toxicity of Other Environmental Toxicants by Heat Shock Proteins

In nematodes, heat shock treatment induced the significant increase in HSP-16.1::GFP, HSP-16.2::GFP, HSP-16.41::GFP, and HSP-16.48::GFP (Fig. 11.8) [28]. Meanwhile, hypoxia treatment also induced the significant increase in HSP-16.1::GFP and HSP-16.2::GFP, and ethanol treatment induced the significant increase in HSP-16.1::GFP, HSP-16.2::GFP, HSP-16.41::GFP, and HSP-16.48::GFP (Fig. 11.8) [28].

Moreover, it was found that mutation of *hsp-16.48* could further result in a susceptibility to the TiO₂-NPs toxicity in reducing body length, in reducing brood size, in decreasing locomotion behavior, and in inducing intestinal autofluorescence and ROS production [18]. Similarly, mutation of *hsp-16.48* caused the susceptibility to graphene oxide (GO) toxicity in reducing brood size, in decreasing locomotion behavior, and in inducing intestinal ROS production, and the enhanced accumulation of GO in the body of nematodes (Fig. 11.9) [29]. In addition, mutation of *hsp-70* or *hsp-3* increased the susceptibility of nematodes to Mn toxicity in reducing lifespan, and mutation of *hsp-70* enhanced neurotoxicity of Mn in inducing the degradation of dopaminergic neurons in nematodes [30].

11.3.3 Regulation of Toxicity of Other Environmental Toxicants by HSF-1

Environmental pathogen infection can potentially cause the toxicity as different aspects on organisms, including the nematodes [31–39]. It was observed that RNAi knockdown of *hsf-1* induced a susceptibility to *P. aeruginosa* PA14 infection in reducing the lifespan, whereas overexpression of HSF-1 induced a resistance to *P.*

Fig. 11.8 (continued) expression of HSP16-1. HSP16-1 is minimally expressed without stress. The second row represents the result of exposure to 7% ethanol for 30 min. The third row represents the result of exposure to 1 mM of sodium azide for 30 min. The forth row represents the result of exposure to 200 mM of NaCl solution for 30 min, and the last row represents the result of starvation for 12 h. The figures of the first and third column are Nomarski images, and the second and fourth are GFP fluorescence driven by the *hsp-16-1* promoter. HSP-16.1 was more strongly induced by starvation than by other stresses and appeared as punctuated spots. The scale bar represents 50 μ m. (b) Hypoxia response of the *hsp-16* genes in a hypoxia chamber. Each column represents the expression of *hsp-16.1*, *hsp-16.2*, *hsp-16.41*, and *hsp-16.48*, respectively. Upper panels are control animals and lower panels, the animals incubated in the hypoxia chamber. Only *hsp-16.1* and *hsp-16.2* responded to hypoxia. (c) Hypoxia response of the *hsp-16* genes in the animals soaked in the M9 buffer. Each column represents the expression of *hsp-16.1*, *hsp-16.2*, *hsp-16.41*, and *hsp-16.48*, respectively. All four genes are responsive to heat shock and ethanol stress, but only *hsp-16.1* and *hsp-16.2* responded to hypoxia. We observed more than 30 animals from at least two independent transgenic lines for each gene and obtained similar results shown in this figure. This figure shows representative animals. The scale bars in (b, c) represent 0.2 mm

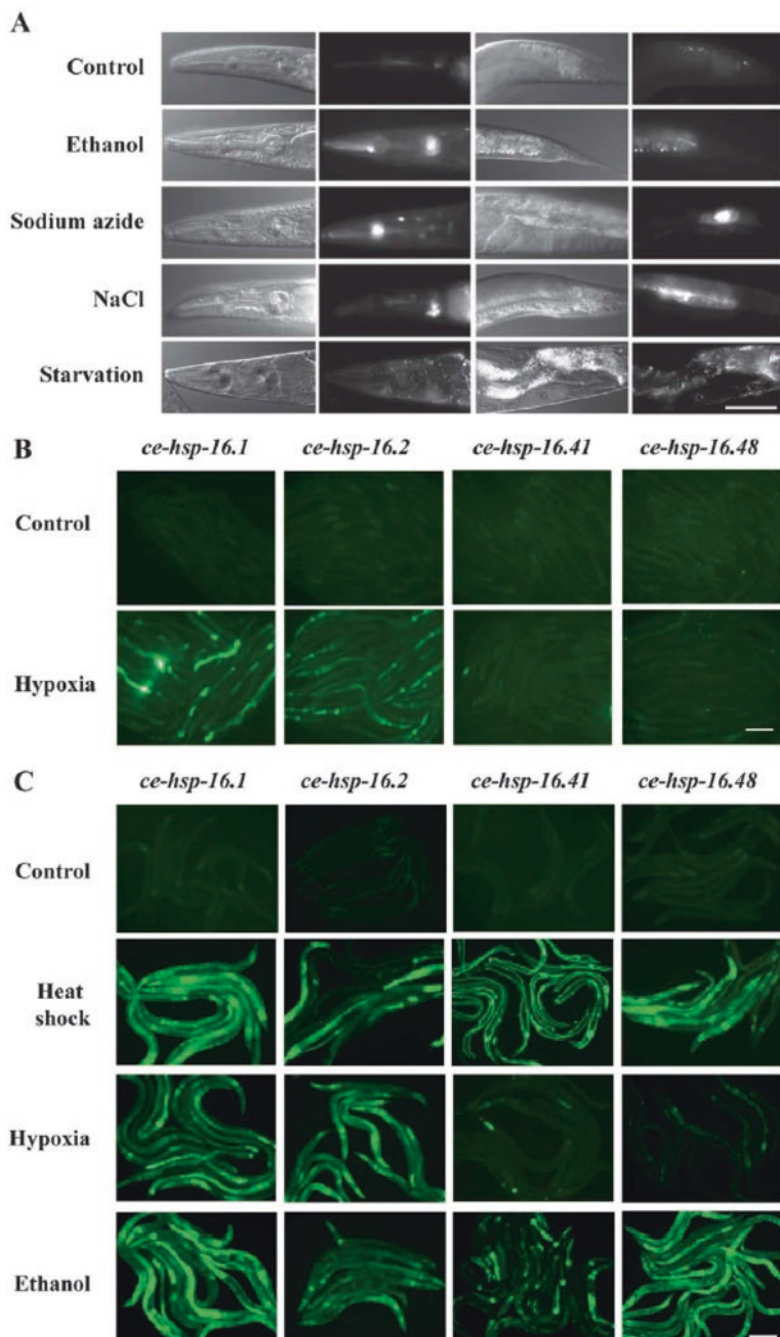


Fig. 11.8 The hypoxia responses of the *hsp-16* genes in *C. elegans* are distinct [28]. (a) The expression of HSP-16.1 is induced by several types of stress. The first row represents the basal

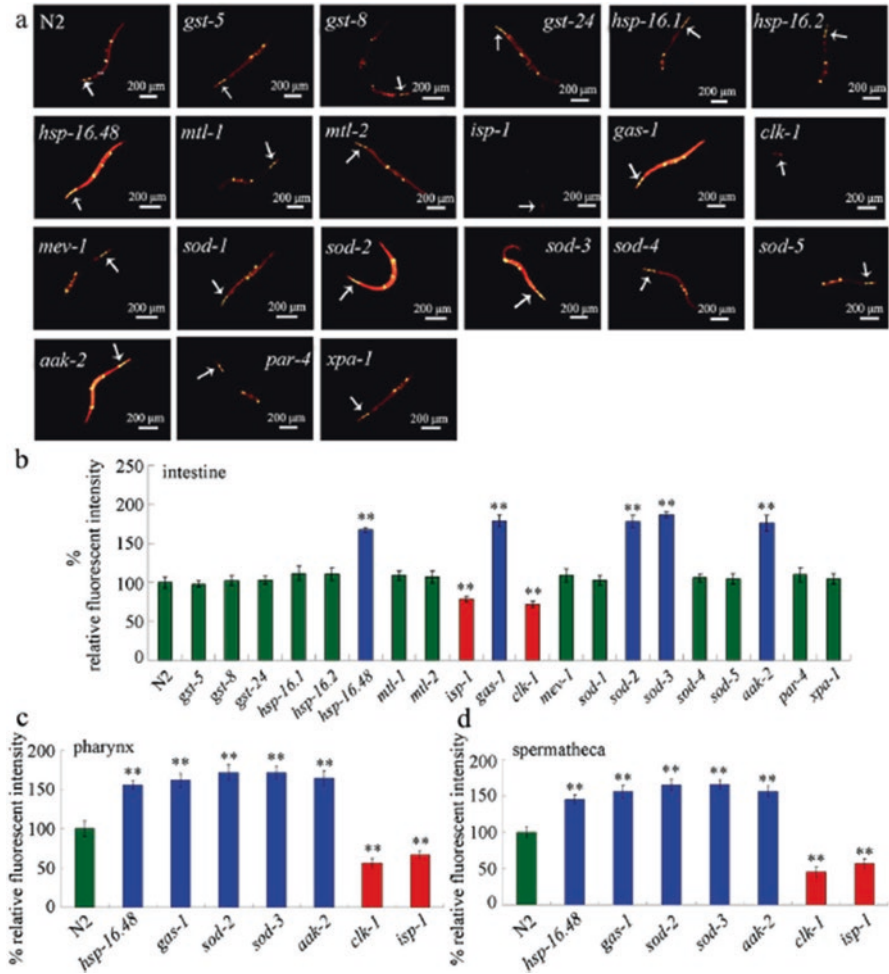


Fig. 11.9 Distributions of GO-Rho B in wild-type and mutant nematodes [29]. (a) Pictures showing the distributions of GO-Rho B in wild-type and mutant nematodes. (b) Comparison of relative fluorescence of GO-Rho B in the intestine between wild-type and mutant nematodes. (c) Comparison of relative fluorescence of GO-Rho B in the pharynx between wild-type and mutant nematodes. (d) Comparison of relative fluorescence of GO-Rho B in the spermatheca between wild-type and mutant nematodes. The arrowheads indicate the pharynx. The intestine (***) and the spermatheca (*) are also indicated. GO exposure was performed from L1-larvae to young adult. The exposure concentration of GO was 100 mg/L. Bars represent means ± SEM. ***P* < 0.01 vs. N2

aeruginosa PA14 infection in reducing the lifespan (Fig. 11.10) [40]. The susceptibility of *hsf-1* mutant nematodes to *P. aeruginosa* PA14 infection in reducing the lifespan could be further enhanced by RNAi knockdown of *pmk-1* encoding a p38 MAPK in p38 MAPK signaling pathway (Fig. 11.10) [40].

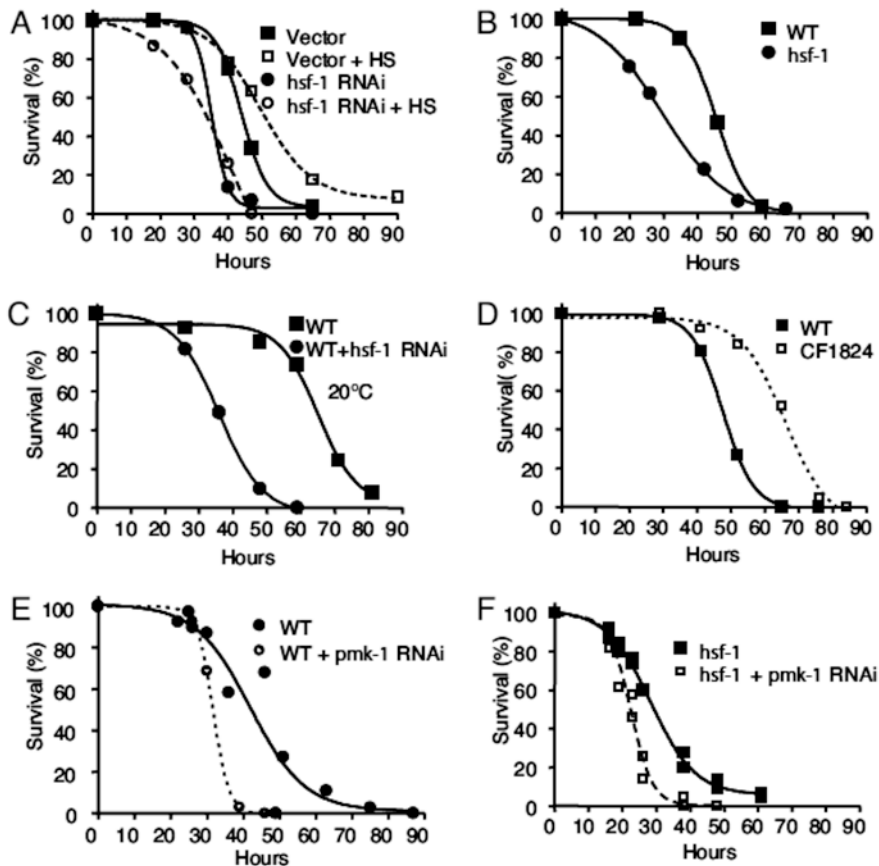


Fig. 11.10 HSF is required for *C. elegans* immunity to *P. aeruginosa* [40]. (a) Wild-type worms grown on *E. coli* carrying a vector control were untreated or HS-treated and exposed to *P. aeruginosa* ($P < 0.03$). In addition, wild-type animals grown on *E. coli* expressing *hsf-1* double-stranded RNA were untreated or HS-treated and exposed to *P. aeruginosa* ($P = 0.2660$). *hsf-1* RNAi animals were more susceptible to *P. aeruginosa* compared with vector RNAi controls ($P < 0.005$). (b) Wild-type or *hsf-1*(*sy441*) animals were grown on *E. coli* carrying a vector control and exposed to *P. aeruginosa* ($P < 0.0001$). (c) Wild-type animals grown on vector control or *hsf-1* double-stranded RNA were exposed to *P. aeruginosa* at 20 °C ($P < 0.0001$). (d) Wild-type or CF1824 (*hsf-1* overexpression) animals were exposed to *P. aeruginosa* ($P < 0.001$). (e) Wild-type animals grown on *E. coli* carrying a vector control or expressing *pmk-1* double-stranded RNA were exposed to *P. aeruginosa* ($P < 0.0001$). (f) *hsf-1*(*sy441*) animals grown on *E. coli* carrying a vector control or expressing *pmk-1* double-stranded RNA were exposed to *P. aeruginosa* ($P = 0.0023$). For each condition, 80–200 animals were used

In nematodes, it was further observed that RNAi knockdown of *hsf-1* could suppress the resistance of *daf-2* mutant nematodes to pathogen infection (Fig. 11.11) [40], suggesting that HSF-1 may act downstream of insulin signaling pathway to regulate the innate immune response to pathogen infection in nematodes. That is,

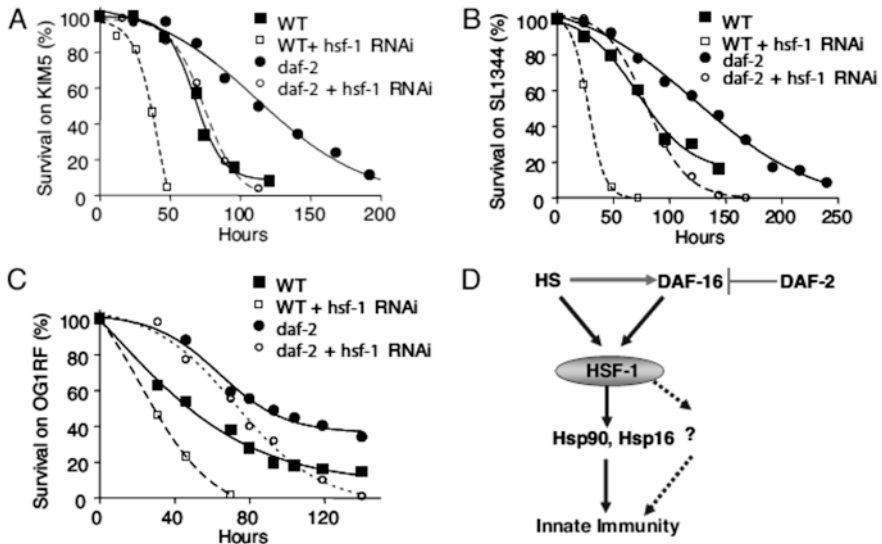


Fig. 11.11 HSF-1 is required for immunity to Gram-negative and Gram-positive pathogens [40]. (a) Wild-type worms grown on *E. coli* carrying a vector control or on *E. coli* expressing *hsf-1* double-stranded RNA were exposed to *Y. pestis* KIM5 ($P < 0.0001$). *daf-2*(*e1370*) worms grown on *E. coli* carrying a vector control or on *E. coli* expressing *hsf-1* double-stranded RNA were exposed to *Y. pestis* KIM5 ($P < 0.001$). (b) Wild-type worms grown on *E. coli* carrying a vector control or on *E. coli* expressing *hsf-1* double-stranded RNA were exposed to *S. enterica* SL1344 ($P < 0.0001$). *daf-2*(*e1370*) worms grown on *E. coli* carrying a vector control or on *E. coli* expressing *hsf-1* double-stranded RNA were exposed to *S. enterica* SL1344 ($P < 0.0001$). (c) Wild-type worms grown on *E. coli* carrying a vector control or on *E. coli* expressing *hsf-1* double-stranded RNA were exposed to *En. faecalis* OG1RF ($P < 0.0001$). *daf-2*(*e1370*) worms grown on *E. coli* carrying a vector control or on *E. coli* expressing *hsf-1* double-stranded RNA also were exposed to *En. faecalis* OG1RF ($P < 0.0001$). (d) HSF-1 activated by HS and the DAF-2_DAF-16 pathway enhances *C. elegans* immunity. HSF-1 mediates protection via induction of Hsp90 and small HSPs in a PMK-1-independent manner

the increased temperature activated HSF-1 will enhance the innate immunity, and this HSF-1 defense response is mediated by the further induction of a system of chaperones.

11.4 Hypoxia Response Signaling

11.4.1 Molecular Signaling for Hypoxia Response

11.4.1.1 HIF-1 and EGL-9

hif-1 encodes a bHLH-PAS hypoxia-inducible transcription factor. During the response to hypoxia stress, a physical complex is formed, and this complex contains HIF-1 and AHA-1, which are encoded by *C. elegans* homologs of hypoxia-inducible factor

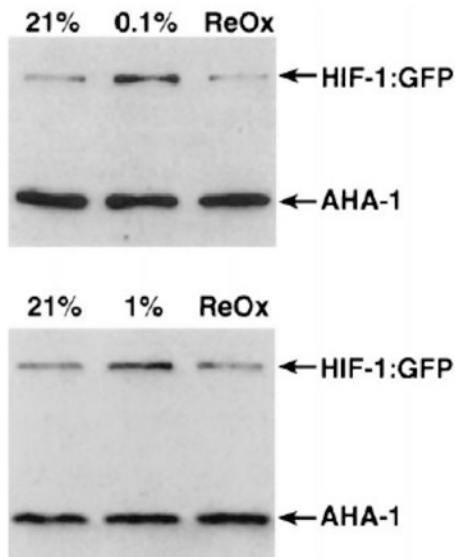


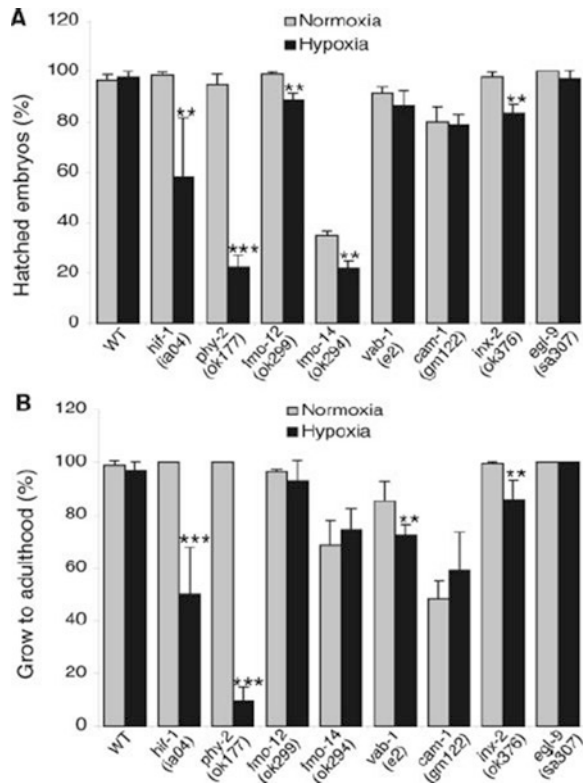
Fig. 11.12 HIF-1:GFP protein levels are increased by hypoxia [41]. The transgenic *C. elegans* strain pHJ06 Ex6, which expresses the complete HIF-1 protein fused to GFP, was harvested before (21% O₂) and after incubation in 0.1% oxygen (*upper*) or 1% oxygen (*lower*) for 8 h. In each experiment, a fraction of the hypoxia-treated worms was reoxygenated for 10 min (ReOx). Worms were lysed by boiling in loading buffer, and equal amounts of total protein were loaded in each lane. The expression of HIF-1:GFP and AHA-1 was assayed by probing the immunoblot with a GFP-specific antibody and the AHA-1-specific mAb 10H8

(HIF) α and β subunits, respectively [41]. The expression of HIF-1:GFP could be highly induced by hypoxia and was subsequently reduced upon reoxygenation (Fig. 11.12) [41]. In addition, the subcellular localization of AHA-1 was disrupted in the *hif-1* (*ia04*) mutant nematodes [41], suggesting that HIF-1 acts upstream of AHA-1 to regulate the hypoxia stress in a complex.

HIF-1 is a critical regulator for the responses to low oxygen levels. The *hif-1* mutant nematodes exhibited no adaptation to hypoxia stress, and the majority of *hif-1*-defective nematodes would die under these conditions (Fig. 11.13) [41, 42]. Additionally, it was found that some HIF-1 target genes could negatively regulate the formation of stress-resistant dauer larvae [42], suggesting the potential involvement of HIF-1 in the regulation of other stresses in nematodes.

A summary for the basics molecular basis for the hypoxia response signaling is provided in Fig. 11.14 [42]. During the control of response to hypoxia stress, EGL-9/PHD modifies the HIF-1, thereby increasing its affinity for VHL-1/E3 ligase to target the HIF-1 for proteasomal degradation (Fig. 11.14) [42]. That is, the proteasomal degradation of HIF-1 is mediated by both the EGL-9 and the VHL-1 (Fig. 11.14) [42]. Meanwhile, the expression of *egl-9* could also be regulated by *hif-1* mutation [42]. This suggests that the positive regulation of *egl-9* transcription by HIF-1 will further help to maintain the EGL-9 activity when oxygen substrate is

Fig. 11.13 Viability assays in normoxia (21% oxygen) and hypoxia (0.5% oxygen) [42]. Animals carrying strong loss-of-function mutations in downstream targets of HIF-1 were incubated in 0.5% oxygen (hypoxia) or room air (normoxia) for 24 h and then assayed for successful completion of embryogenesis (a) and survival to adulthood (b). Asterisks indicate that the viability of hypoxia-treated mutants is significantly lower than that of wild-type (WT)

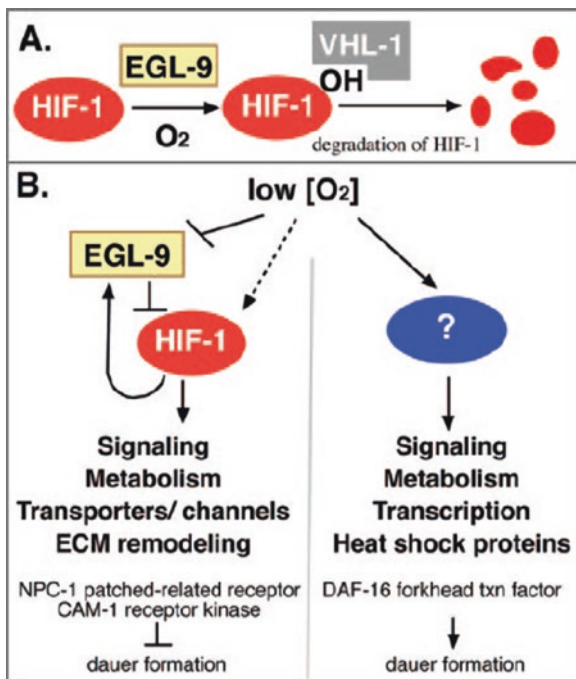


limiting, and a feedback loop will be activated to attenuate the HIF-1 activation (Fig. 11.14) [42]. In addition, the response to hypoxia is mediated by HIF-1-dependent or by HIF-1-independent pathway(s) (Fig. 11.14) [42]. HIF-1 can further positively regulate the expression of *npc-1* and *cam-1*, regulators of dauer formation [42]. The increased expression in *daf-16* is a common feature of the hypoxia response and of the perturbations in insulin signaling pathway [42].

11.4.1.2 Aminoacyl-tRNA Synthetase RRT-1

rrt-1 encodes a arginyl-transfer RNA (tRNA) synthetase, an enzyme essential for protein translation. Mutation or RNAi knockdown of *rrt-1* or other genes encoding the aminoacyl-tRNA synthetase could rescue the nematodes from the hypoxia-induced death [43]. More importantly, this hypoxia resistance was inversely correlated with the protein translation rate [43]. The ER unfolded protein response (UPR) induced by hypoxia was required for the resistance of *rrt-1* mutant nematodes to the hypoxia stress [43], suggesting that the translational suppression can induce the hypoxia resistance in part by reducing the unfolded protein toxicity in nematodes.

Fig. 11.14 Models for hypoxia signaling and response [42]



11.4.2 Regulation of Toxicity of Other Environmental Toxicants by HIF-1 and EGL-9

In nematodes, it was found that loss-of-function mutation of *hif-1* promoted the resistance of nematodes to exogenous mitochondrial stressor ethidium bromide (EtBr) and suppressed the EtBr-induced ROS production (Fig. 11.15) [44]. Similarly, mutation of *hif-1* also induced a resistance to high-glucose diets stress in reducing lifespan in nematodes [45]. During the control of EtBr toxicity, p38 MAPK signaling was identified as an indispensable factor for the survival against mitochondrial stress in *hif-1* mutant nematodes [45].

Moreover, it was observed that mutation of *hif-1* induced a susceptibility to pore-forming toxins (PFTs) toxicity in reducing the lifespan (Fig. 11.16) [46]. In contrast, the Cry21A PFT resistance was observed in *egl-9* mutant nematodes (Fig. 11.16) [46]. In nematodes, the intestinal specific expression of *egl-9* was sufficient to rescue the Cry21A PFT resistance [46]. Two of the downstream effectors of this pathway were identified, and they were nuclear receptor NHR-57- and XBP-1-mediated ER UPR signaling during the control of PFTs toxicity in nematodes.

Furthermore, it was found that mutation of *hif-1* induced a susceptibility to pathogen infection, whereas mutation of *egl-9* induced a resistance to pathogen infection (Fig. 11.17) [47]. Moreover, the HIF-1 α was dispensable for the host defense gene induction, and SWAN-1-mediated noncanonical pathway inhibited this HIF-1 induced defense gene repression in nematodes [47].

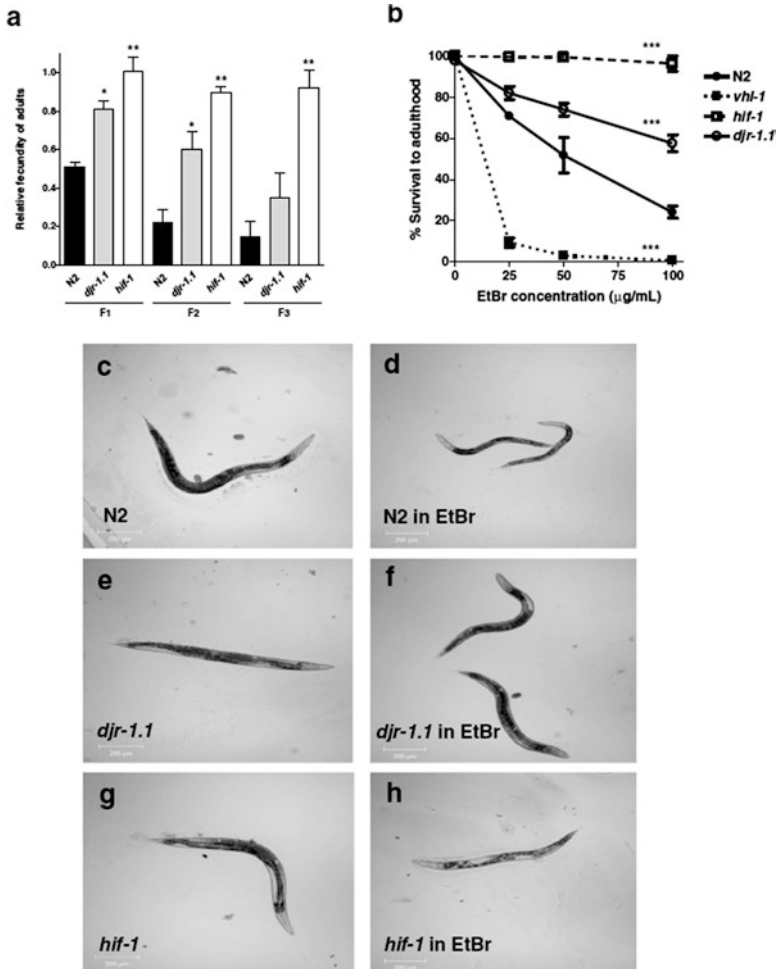
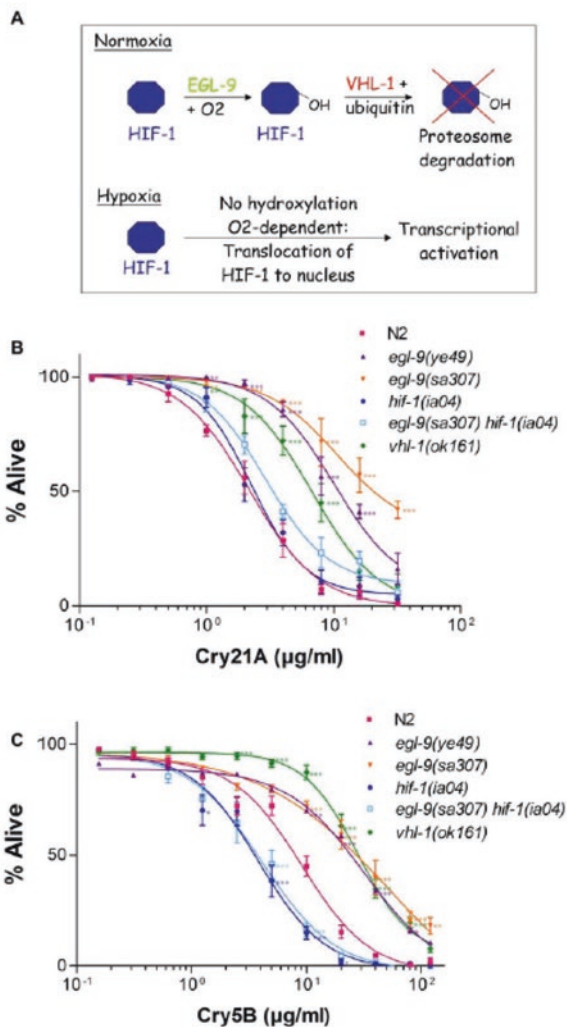


Fig. 11.15 *hif-1* and *djr-1.1* mutants are highly resistant to EtBr [44]. (a) *hif-1* animals exposed to EtBr have no effect on fecundity over three generations, while wild-type worms showed a significant decrease in brood size. Brood size of N2 (wild-type), *djr-1.1*, and *hif-1* animals in 25 μg/mL EtBr were counted for three generations: F1, F2, and F3. Relative fecundity is measured as the number of progeny grown to adulthood on EtBr divided by the number of progeny grown to adulthood in the absence of EtBr and would include animals that arrest at the L3 stage. Animals with ruptured vulva were not counted. Asterisk marks denote significant difference of fecundity between P0 (normalized to 1.0) and the following generations for each strain (* denotes $p < 0.05$ and ** $p < 0.01$) using one-way ANOVA. (b) Concentration dependence of EtBr. N2, *hif-1*, *vhl-1*, and *djr-1.1* mutant animals (first generation) were grown on worm plates containing nematode growth media and various concentrations of EtBr (0, 25, 50, and 100 μg/mL). The number of worms that grew to adulthood was determined and plotted. To determine significant differences over different concentrations of EtBr, the data were subjected to two-way ANOVA comparing groups (different strains) over different concentrations of EtBr. All strains showed a significant difference compared to N2 (***) ($p < 0.001$). (c–h) Growth of strains on EtBr. N2, *djr-1.1* and *hif-1* worms (as labeled) 4 days after egg-laying in plates containing either no EtBr (c, e, g) or 50 μg/mL EtBr (d, f, h)

Fig. 11.16 Quantitative response of *egl-9* and HIF-1 pathway mutants to Cry PFTs [46]. (a) Schematic illustrating O₂-dependent regulation of HIF-1 activity. The O₂-dependent prolyl hydroxylation of HIF-1 by EGL-9/PHD increases its affinity to VHL-1, leading to ubiquitylation and destruction. (b, c) Dose-dependent mortality assays were performed using (b) Cry21A spore crystal lysates or (c) purified Cry5B to quantitatively compare sensitivities of wild-type N2, *egl-9* mutants, and HIF-1 pathway mutants to PFTs. Each data point shows the mean and standard errors of the mean of results from three independent experiments (three wells per experiment; on average, 180 animals per data point). Statistical differences between mutant strains and N2 are given for each concentration using P values represented by asterisks as follows: * *P* < 0.05; ** *P* < 0.01; *** *P* < 0.001



11.5 Perspectives

In this chapter, we selected three well-described response signals (heavy metal response, heat shock response, and hypoxia response) to discuss the question on the specificity of molecular signals in response to certain environmental toxicants or stresses in nematodes. Actually, there are still other relevant evidence on the study of UV irradiation, osmotic stress, etc. As introduced and discussed in this chapter, so far the obtained data in nematodes does not support the existence of specific molecular signals in response to certain environmental toxicants or stresses. The molecular basis for the response to heavy metal response, heat shock response, or

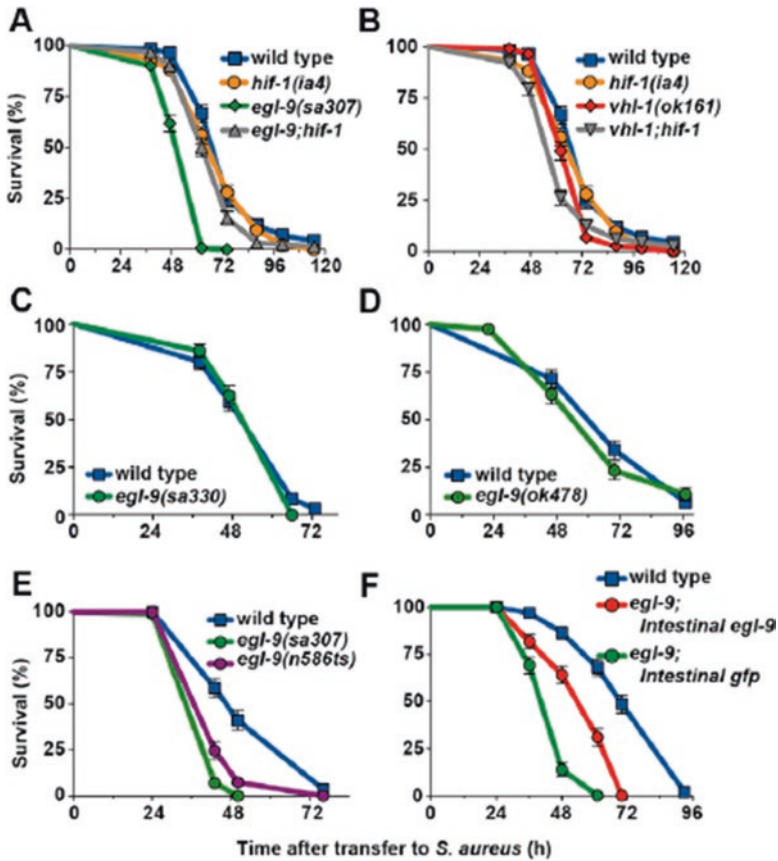


Fig. 11.17 *egl-9* inactivation causes enhanced susceptibility to *S. aureus*-mediated killing [47]. (a) *egl-9(sa307)* animals exhibited enhanced susceptibility, whereas *egl-9(sa307);hif-1(ia4)* mutants exhibited near wild-type susceptibility. Survival analysis: *egl-9* Kaplan–Meier median survival (MS) = 62 h, time to 50% death by nonlinear regression analysis (LT50) = 48.78 h, number of animals (N) = 142, $p < 0.0001$ (log-rank test, compared with wild-type); *egl-9;hif-1* MS = 68 h, LT50 = 62.10 h, $N = 122/2$, $p = 0.0030$ (compared with wild-type). (b) *vhl-1(ok161)* and *hif-1(ia4)* animals exhibited near wild-type susceptibility. Survival analysis: wild-type MS = 74 h, LT50 = 67.03 h, $N = 117/5$; *vhl-1* MS = 62 h, LT50 = 61.86 h, $N = 118$, $p < 0.0001$ (compared with wild-type); *hif-1* MS = 74 h, LT50 = 64.77 h, $N = 136$, $p = 0.0943$ (compared with wild-type). (c) *egl-9(sa330)* animals and (d) *egl-9(ok478)* animals exhibit wild-type susceptibility. (e) *egl-9(n586ts)* animals are hypersusceptible to *S. aureus*. Survival analysis: *egl-9(sa307)* MS = 43 h, $N = 95/1$, $p < 0.0001$ (compared with wild-type); *egl-9(n586ts)* MS = 43 h, $N = 96/15$, $p < 0.0001$ (compared with wild-type); wild-type MS = 50 h, $N = 92/9$. (f) Wild-type, *egl-9(sa307);crp-1::egl-9* (Intestinal *egl-9*), and *egl-9(sa307);crp-1::gfp* (Intestinal *gfp*) animals show that intestinal expression of EGL-9, but not GFP, rescues the *egl-9(sa307)* enhanced susceptibility phenotype. Survival analysis: wild-type MS = 70 h, $N = 108/7$; Intestinal *egl-9* MS = 61 h, $N = 115/14$, $p < 0.0001$ (compared with wild-type), $p < 0.0001$ (compared with Intestinal *gfp*); Intestinal *gfp* MS = 48 h, $N = 102/3$, $p < 0.0001$ (compared with wild-type). Results are representative of two independent trials, performed in triplicate. Animals were subjected to *cdc-25* RNAi to prevent reproduction and subsequently transferred to *S. aureus* killing assay plates

hypoxia response can also involve in the regulation of toxicity of other environmental toxicants or stresses under certain conditions. However, this also not means that the nematodes share the completely same molecular signaling pathways in response to different environmental toxicants or stresses. The further studies are suggested to focus on the definition of direct or primary molecular signals involved in the regulation of certain environmental toxicants or stresses in nematodes.

References

1. Wang D-Y (2018) Nanotoxicology in *Caenorhabditis elegans*. Springer, Singapore
2. Li W-J, Wang D-Y, Wang D-Y (2018) Regulation of the response of *Caenorhabditis elegans* to simulated microgravity by p38 mitogen-activated protein kinase signaling. *Sci Rep* 8:857
3. Xiao G-S, Zhao L, Huang Q, Yang J-N, Du H-H, Guo D-Q, Xia M-X, Li G-M, Chen Z-X, Wang D-Y (2018) Toxicity evaluation of Wanzhou watershed of Yangtze Three Gorges Reservoir in the flood season in *Caenorhabditis elegans*. *Sci Rep* 8:6734
4. Xiao G-S, Zhao L, Huang Q, Du H-H, Guo D-Q, Xia M-X, Li G-M, Chen Z-X, Wang D-Y (2018) Biosafety assessment of water samples from Wanzhou watershed of Yangtze Three Gorges Reservoir in the quiet season in *Caenorhabditis elegans*. *Sci Rep* 8:14102
5. Yin J-C, Liu R, Jian Z-H, Yang D, Pu Y-P, Yin L-H, Wang D-Y (2018) Di (2-ethylhexyl) phthalate-induced reproductive toxicity involved in DNA damage-dependent oocyte apoptosis and oxidative stress in *Caenorhabditis elegans*. *Ecotoxicol Environ Saf* 163:298–306
6. Wu Q-L, Han X-X, Wang D, Zhao F, Wang D-Y (2017) Coal combustion related fine particulate matter (PM_{2.5}) induces toxicity in *Caenorhabditis elegans* by dysregulating microRNA expression. *Toxicol Res* 6:432–441
7. Swain SC, Keusekotten K, Baumeister R, Sturzenbaum SR (2004) *C. elegans* metallothioneins: new insights into the phenotypic effects of cadmium toxicosis. *J Mol Biol* 341:951–959
8. Liao VH, Dong J, Freedman JH (2002) Molecular characterization of a novel, cadmium-inducible gene from the nematode *Caenorhabditis elegans*. *J Biol Chem* 277:42049–42069
9. Hall J, Haas KL, Freedman JH (2012) Role of MTL-1, MTL-2, and CDR-1 in mediating cadmium sensitivity in *Caenorhabditis elegans*. *Toxicol Sci* 128:418–426
10. Ren M-X, Zhao L, Ding X-C, Krasteva N, Rui Q, Wang D-Y (2018) Developmental basis for intestinal barrier against the toxicity of graphene oxide. *Part Fibre Toxicol* 15:26
11. Xiao G-S, Chen H, Krasteva N, Liu Q-Z, Wang D-Y (2018) Identification of interneurons required for the aversive response of *Caenorhabditis elegans* to graphene oxide. *J Nanobiotechnol* 16:45
12. Ding X-C, Rui Q, Wang D-Y (2018) Functional disruption in epidermal barrier enhances toxicity and accumulation of graphene oxide. *Ecotoxicol Environ Saf* 163:456–464
13. Zhao L, Kong J-T, Krasteva N, Wang D-Y (2018) Deficit in epidermal barrier induces toxicity and translocation of PEG modified graphene oxide in nematodes. *Toxicol Res* 7(6):1061–1070. <https://doi.org/10.1039/C8TX00136G>
14. Qu M, Xu K-N, Li Y-H, Wong G, Wang D-Y (2018) Using *acs-22* mutant *Caenorhabditis elegans* to detect the toxicity of nanopolystyrene particles. *Sci Total Environ* 643:119–126
15. Dong S-S, Qu M, Rui Q, Wang D-Y (2018) Combinational effect of titanium dioxide nanoparticles and nanopolystyrene particles at environmentally relevant concentrations on nematodes *Caenorhabditis elegans*. *Ecotoxicol Environ Saf* 161:444–450
16. Xiao G-S, Zhi L-T, Ding X-C, Rui Q, Wang D-Y (2017) Value of *mir-247* in warning graphene oxide toxicity in nematode *Caenorhabditis elegans*. *RSC Adv* 7:52694–52701

17. Zhao L, Wan H-X, Liu Q-Z, Wang D-Y (2017) Multi-walled carbon nanotubes-induced alterations in microRNA *let-7* and its targets activate a protection mechanism by conferring a developmental timing control. *Part Fibre Toxicol* 14:27
18. Rui Q, Zhao Y-L, Wu Q-L, Tang M, Wang D-Y (2013) Biosafety assessment of titanium dioxide nanoparticles in acutely exposed nematode *Caenorhabditis elegans* with mutations of genes required for oxidative stress or stress response. *Chemosphere* 93:2289–2296
19. Polak N, Read DS, Jurkschat K, Matzke M, Kelly FJ, Spurgeon DJ, Stürzenbaum SR (2014) Metalloproteins and phytochelatin synthase may confer protection against zinc oxide nanoparticle induced toxicity in *Caenorhabditis elegans*. *Comp Biochem Physiol C* 160:75–85
20. Zhao L, Qu M, Wong G, Wang D-Y (2017) Transgenerational toxicity of nanopolystyrene particles in the range of $\mu\text{g/L}$ in nematode *Caenorhabditis elegans*. *Environ Sci Nano* 4:2356–2366
21. Shao H-M, Han Z-Y, Krasteva N, Wang D-Y (2018) Identification of signaling cascade in the insulin signaling pathway in response to nanopolystyrene particles. *Nanotoxicology in press*
22. Murphy CT, McCarroll SA, Bargmann CI, Fraser A, Kamath RS, Ahringer J, Li H, Kenyon C (2003) Gene that act downstream of DAF-16 to influence the lifespan of *Caenorhabditis elegans*. *Nature* 424:277–284
23. Pinkston-Gosse J, Kenyon C (2007) DAF-16/FOXO targets genes that regulate tumor growth in *Caenorhabditis elegans*. *Nat Genet* 39:1403–1409
24. Tepper RG, Ashraf J, Kaletsky R, Kleemann G, Murphy CT, Bussemaker HJ (2013) PQM-1 complements DAF-16 as a key transcriptional regulator of DAF-2-mediated development and longevity. *Cell* 154:676–690
25. Snutch TP, Baillie DL (1983) Alterations in the pattern of gene expression following heat shock in the nematode *Caenorhabditis elegans*. *Can J Biochem Cell Biol* 61:480–487
26. Morley JF, Morimoto RL (2004) Regulation of longevity in *Caenorhabditis elegans* by heat shock factor and molecular chaperones. *Mol Biol Cell* 15:657–664
27. Hajdu-Cronin YM, Chen WJ, Sternberg PW (2004) The L-type cyclin CYL-1 and the heat-shock-factor HSF-1 are required for heat-shock-induced protein expression in *Caenorhabditis elegans*. *Genetics* 168:1937–1949
28. Hong M, Kwon JY, Shim J, Lee J (2004) Differential hypoxia response of *hsp-16* genes in the nematode. *J Mol Biol* 344:369–381
29. Wu Q-L, Zhao Y-L, Li Y-P, Wang D-Y (2014) Molecular signals regulating translocation and toxicity of graphene oxide in nematode *Caenorhabditis elegans*. *Nanoscale* 6:11204–11212
30. Avila DS, Benedetto A, Au C, Bornhorst J, Aschner M (2016) Involvement of heat shock proteins on Mn induced toxicity in *Caenorhabditis elegans*. *BMC Pharmacol Toxicol* 17:54
31. Zhi L-T, Yu Y-L, Li X-Y, Wang D-Y, Wang D-Y (2017) Molecular control of innate immune response to *Pseudomonas aeruginosa* infection by intestinal *let-7* in *Caenorhabditis elegans*. *PLoS Pathog* 13:e1006152
32. Zhi L-T, Yu Y-L, Jiang Z-X, Wang D-Y (2017) *mir-355* functions as an important link between p38 MAPK signaling and insulin signaling in the regulation of innate immunity. *Sci Rep* 7:14560
33. Sun L-M, Liao K, Hong C-C, Wang D-Y (2017) Honokiol induces reactive oxygen species-mediated apoptosis in *Candida albicans* through mitochondrial dysfunction. *PLoS ONE* 12:e0172228
34. Sun L-M, Liao K, Wang D-Y (2017) Honokiol induces superoxide production by targeting mitochondrial respiratory chain complex I in *Candida albicans*. *PLoS ONE* 12:e0184003
35. Sun L-M, Zhi L-T, Shakoos S, Liao K, Wang D-Y (2016) microRNAs involved in the control of innate immunity in *Candida* infected *Caenorhabditis elegans*. *Sci Rep* 6:36036
36. Sun L-M, Liao K, Li Y-P, Zhao L, Liang S, Guo D, Hu J, Wang D-Y (2016) Synergy between PVP-coated silver nanoparticles and azole antifungal against drug-resistant *Candida albicans*. *J Nanosci Nanotechnol* 16:2325–2335

37. Wu Q-L, Cao X-O, Yan D, Wang D-Y, Aballay A (2015) Genetic screen reveals link between maternal-effect sterile gene *mes-1* and *P. aeruginosa*-induced neurodegeneration in *C. elegans*. *J Biol Chem* 290:29231–29239
38. Yu Y-L, Zhi L-T, Guan X-M, Wang D-Y, Wang D-Y (2016) FLP-4 neuropeptide and its receptor in a neuronal circuit regulate preference choice through functions of ASH-2 trithorax complex in *Caenorhabditis elegans*. *Sci Rep* 6:21485
39. Yu Y-L, Zhi L-T, Wu Q-L, Jing L-N, Wang D-Y (2018) NPR-9 regulates innate immune response in *Caenorhabditis elegans* by antagonizing activity of AIB interneurons. *Cell Mol Immunol* 15:27–37
40. Singh V, Aballay A (2006) Heat-shock transcription factor (HSF)-1 pathway required for *Caenorhabditis elegans* immunity. *Proc Natl Acad Sci U S A* 103:13092–13097
41. Jiang H, Guo R, Powell-Coffman JA (2001) The *Caenorhabditis elegans hif-1* gene encodes a bHLH-PAS protein that is required for adaptation to hypoxia. *Proc Natl Acad Sci U S A* 98:7916–7921
42. Shen C, Nettleton D, Jiang M, Kim SK, Powell-Coffman JA (2005) Roles of the HIF-1 hypoxia-inducible factor during hypoxia response in *Caenorhabditis elegans*. *J Biol Chem* 280:20580–20588
43. Anderson LL, Mao X, Scott BA, Crowder CM (2009) Survival from hypoxia in *C. elegans* by inactivation of aminoacyl-tRNA synthetases. *Science* 323:630–633
44. Kamal M, D'Amora DR, Kubiseski TJ (2016) Loss of *hif-1* promotes resistance to the exogenous mitochondrial stressor ethidium bromide in *Caenorhabditis elegans*. *BMC Cell Biol* 17:34
45. AlcaÂntar-FernaÂndez J, Navarro RE, Salazar-MartÃ³nez AM, PeÃ±ez-Andrade ME, Miranda-RÃ³os J (2018) *Caenorhabditis elegans* respond to high-glucose diets through a network of stress- responsive transcription factors. *PLoS ONE* 13:e0199888
46. Bellier A, Chen C-S, Kao C-Y, Cinar HN, Aroian RV (2009) Hypoxia and the hypoxic response pathway protect against pore-forming toxins in *C. elegans*. *PLoS Pathog* 5:e1000689
47. Luhachack LG, Visvikis O, Wollenberg AC, Lacy-Hulbert A, Stuart LM, Irazoqui JE (2012) EGL-9 controls *C. elegans* host defense specificity through prolyl hydroxylation-dependent and -independent HIF-1 pathways. *PLoS Pathog* 8:e1002798